Ultrasound-guided tissue fractionation by high intensity focused ultrasound in an in vivo porcine liver model

Tatiana D. Khokhlova[a,b,1], Yak-Nam Wang[b], Julianna C. Simon[b], Bryan W. Cunitz[b], Frank Starr[b], Marla Paun[b], Lawrence A. Crum[b], Michael R. Bailey[b], and Vera A. Khokhlova[b,c]

[a]Division of Gastroenterology, Department of Medicine, University of Washington, Seattle, WA 98195; [b]Center for Industrial and Medical Ultrasound, Applied Physics Laboratory, University of Washington, Seattle, WA 98105; and [c]Department of Acoustics, Physics Faculty, Moscow State University, Leninskie Gory, Moscow 119991, Russia

Edited* by Floyd Dunn, University of Illinois, Urbana, IL, and approved April 28, 2014 (received for review September 27, 2013)

The clinical use of high intensity focused ultrasound (HIFU) therapy for noninvasive tissue ablation has been recently gaining momentum. In HIFU, ultrasound energy from an extracorporeal source is focused within the body to ablate tissue at the focus while leaving the surrounding organs and tissues unaffected. Most HIFU therapies are designed to use heating effects resulting from the absorption of ultrasound by tissue to create a thermally coagulated treatment volume. Although this approach is often successful, it has its limitations, such as the heat sink effect caused by the presence of a large blood vessel near the treatment area or heating of the ribs in the transcostal applications. HIFU-induced bubbles provide an alternative means to destroy the target tissue by mechanical disruption or, at its extreme, local fractionation of tissue within the focal region. Here, we demonstrate the feasibility of a recently developed approach to HIFU-induced ultrasound-guided tissue fractionation in an in vivo pig model. In this approach, termed boiling histotripsy, a millimeter-sized boiling bubble is generated by ultrasound and further interacts with the ultrasound field to fractionate porcine liver tissue into subcellular debris without inducing further thermal effects. Tissue selectivity, demonstrated by boiling histotripsy, allows for the treatment of tissue immediately adjacent to major blood vessels and other connective tissue structures. Furthermore, boiling histotripsy would benefit the clinical applications, in which it is important to accelerate resorption or passage of the ablated tissue volume, diminish pressure on the surrounding organs that causes discomfort, or insert openings between tissues.

High intensity focused ultrasound (HIFU) therapy is a noninvasive ablation method in which ultrasound energy from an extracorporeal source is focused within the body to locally ablate tissue at the focus without damaging surrounding tissues (1, 2). HIFU is most widely used to thermally ablate a variety of both benign and malignant tumors including uterine fibroids, prostate cancer, liver tumors, and other solid tumors that are accessible to ultrasound energy (3–6). It has been shown that HIFU therapy improves survival rates in certain oncological applications and improves outcomes in the treatment of benign conditions (1, 5). Unlike other ablation modalities, such as radiofrequency (RF) or laser ablation, HIFU is completely noninvasive, yet can be used to target deep tissue, which is particularly important in the treatment of many brain disorders. The results of a recent clinical trial of transcranial HIFU for the successful treatment of essential tremor in 15 patients is an incredible milestone demonstrating the potential of this technology (7). HIFU targeting is usually performed by using either magnetic resonance (MR) imaging or B-mode ultrasound imaging (3, 8). Neither method allows for direct visualization of the treated volume; however, MR thermometry is capable of providing tissue temperature maps during treatment, which can be correlated to the thermal dose and permits the ablated tissue volume to be calculated.

In recent years, attention has been drawn to the use of HIFU-induced bubble formation for mechanical tissue disruption so as to facilitate drug delivery to tumors, or to temporarily open the blood–brain barrier (9, 10). At its extreme, bubble activity can cause complete homogenization (liquefaction) of tissue. In particular, controllable, localized ex vivo tissue lysis has been achieved through the generation of a millimeter-size boiling bubble and its interaction with the HIFU field (11). The underlying physical mechanism can be described as follows: When high acoustic pressure waves propagate through water or tissue to the focus, nonlinear effects lead to the transformation of the initial sine wave generated by the transducer into a sawtooth-shaped shock wave in the focal region. Absorption of ultrasound energy at the shock front is very large, because the shock contains a large number of higher harmonics of the operational frequency and absorption in tissue increases with frequency (2). In strongly focused HIFU beams, the shock fronts typically form within the focal region; therefore, enhanced and efficient heating occurs only at the focus, leading to temperatures more than 100 °C, superheated tissue, and explosive localized boiling. This localized boiling can occur in as short a time as a few milliseconds (12). The resultant explosion of the millimeter-sized boiling bubble, and its subsequent interaction with the incoming shocks, cause mechanical erosion of the tissue in the focal region and

Significance

High intensity focused ultrasound (HIFU) therapy is a promising, clinically adopted method of noninvasive tissue ablation used to treat both benign and malignant conditions. This work presents, to our knowledge, the first in vivo validation of a previously developed HIFU-based method that allows for noninvasive fractionation of targeted tissue into subcellular debris—boiling histotripsy—in a large animal model. While fractionating the targeted soft tissue, boiling histotripsy is shown to spare the adjacent connective tissue structures such as blood vessels. The process can be readily targeted and monitored by B-mode ultrasound. The resulting tissue debris are liquid, which provides a potential clinical benefit over thermal ablation in the treatment of tumors that exert uncomfortable pressure on surrounding tissues.

Author contributions: L.A.C., M.R.B., and V.A.K. designed research; T.D.K., Y.-N.W., J.C.S., B.W.C., F.S., M.P., and M.R.B. performed research; T.D.K., Y.-N.W., and V.A.K. analyzed data; and T.D.K., Y.-N.W., J.C.S., and V.A.K. wrote the paper.

The authors declare no conflict of interest.

*This Direct Submission article had a prearranged editor.

[1]To whom correspondence should be addressed. E-mail: tdk7@uw.edu.

This article contains supporting information online at www.pnas.org/lookup/suppl/doi:10.1073/pnas.1318355111/-/DCSupplemental.

ultimately its complete fractionation (11). When the HIFU pulse parameters are controlled so that the pulse length is not much longer than the time to boil, t_b, and the pulse repetition frequency is low enough to avoid heat accumulation, thermal injury to tissue is negligible. As demonstrated in our previous work, the result of the pulsing protocol shown in Fig. 1*B* in ex vivo tissues was a void filled with cell homogenate with no signs of thermal damage to the tissue surrounding the void (13). The current understanding of the mechanism through which the millimeter-sized boiling bubble disrupts tissue into submicron-sized fragments is that a miniature acoustic fountain forms inside the boiling bubble because of the pressure release interface (tissue-vapor) encountered by incoming HIFU shock waves (Fig. 1*C*) (14). Capillary instabilities and cavitation within the fountain leads to tissue atomization, which is similar to the process of water atomization in ultrasonic air humidifiers (14).

We term the approach described above as "boiling histotripsy," in contrast to the previously reported HIFU procedure called "histotripsy," in which much shorter (microsecond- as opposed to millisecond-duration) pulses are used to generate a cavitation cloud in tissue and the activity of the cloud (as opposed to a boiling bubble) is used for tissue erosion (15). Cavitation-cloud histotripsy has been recently demonstrated in vivo for the fragmentation of rabbit kidney (16), canine prostate (17), and porcine liver (18). The treatment was shown to be well tolerated; however, to achieve the focal peak negative pressures sufficient for cavitation cloud formation, very large and highly focused (f-number 0.8) transducers are required, as well as the amplifiers capable of providing extremely high instantaneous power (on the order of several kilowatts). Boiling histotripsy requires significantly less power (on the order of hundreds of watts), making it possible to implement it clinically by using commercially available HIFU systems (19, 20). Moreover, the requirements on the size, focusing gain (f-number 1), and frequency of the HIFU source are less restrictive, which is an advantage when only a limited acoustic window is available. It has also been shown that both boiling histotripsy and cavitation cloud histotripsy procedures can be targeted and monitored with B-mode ultrasound, because both boiling bubbles and cavitation bubble clouds are highly reflective (11).

The first goal of this study was to investigate the feasibility of the boiling histotripsy treatment in vivo in a large animal model under ultrasound image guidance. The second goal was to validate in vivo the approach to the choice of the treatment protocol parameters (e.g., pulse duration, duty factor, focal pressure levels), which was proposed in our prior ex vivo studies (11). The latter aim required the side-by-side comparison of the outcomes of the different boiling histotripsy protocols in vivo and ex vivo in terms of the lesion size, shape, and content.

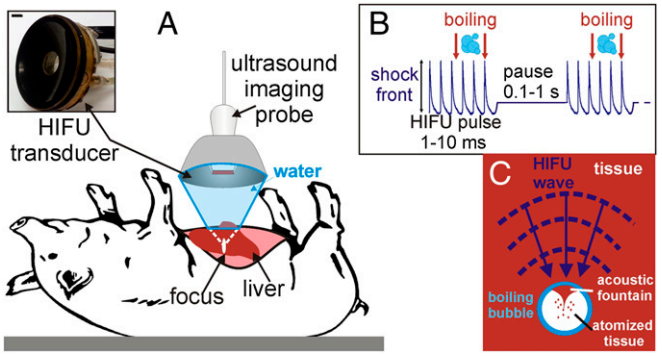

Fig. 1. Illustration of the experimental setup and the physical principle of the HIFU-induced boiling-histotripsy procedure. (*A*) A hand-held 2 MHz HIFU transducer (*Inset*), was attached to a water-filled coupling cone, that was brought into contact with exposed liver of a 100- to 150-lb domestic swine. (Scale bar: 1 cm.) The ultrasound imaging probe was inserted through the central opening of the transducer for targeting and monitoring of the exposure. The HIFU focus was placed at depths of 5–18 mm below the tissue surface. (*B*) The idea behind boiling-histotripsy exposures is to make use of highly nonlinear ultrasound waves that form at the HIFU focus and contain shock fronts. Ultrasound absorption at the shock fronts in tissue is very efficient, which leads to temperature elevations up to 100 °C in a matter of milliseconds in a very small volume around the focus, where shocks are present. A large boiling bubble then forms at the HIFU focus, and its interaction with the remainder of the incident HIFU pulse leads to tissue fractionation. To avoid thermal effects on tissue, short HIFU pulses (1–10 ms) and long intervals between the pulses (0.1–1 s) were used. Each exposure lasted for 50 s, and then the transducer was moved to another spot on the liver. (*C*) Explosive growth of the millimeter-sized boiling bubble and its interaction with the HIFU field causes the breakdown of tissue into submicrometer fragments. The hypothesized physical mechanism behind tissue fractionation is the formation of a miniature acoustic fountain within the boiling bubble and ultrasound-induced tissue atomization.

Results

A hand-held 2-MHz focused ultrasound transducer with a 64-mm diameter and radius of curvature was operated at the acoustic output power of 240 W to provide an in situ focal pressure waveform with an 87–102 MPa shock front (Fig. S1). Different pulsing schemes with 1- to 500-ms-long pulses and 0.1–10 Hz repetition rate (duty factor was kept constant at 0.01) were applied for 50 s to produce boiling histotripsy lesions with varying degrees of thermal damage in the livers of 100- to 150-pound domestic swine. The transducer had a central opening that allowed for coaxial positioning of an ultrasound imaging probe (ATL P4-2 probe, used with Phillips HDI-5000 imaging system) for targeting and treatment guidance. The liver was externalized before the HIFU treatment, and the transducer was attached to a water-coupling cone, sealed with an elastic membrane, and brought into direct contact with the liver lobe, as shown in Fig. 1 and Fig. S2. The externalization was done for precise localization and characterization of the lesions after treatment—the position of the coupling cone was marked with ink on the liver surface after each exposure. Several (two to five) exposures were performed at distinct locations on one of the liver lobes. With variability in liver lobe thickness, the focal depth varied within 5–18 mm by changing the water pressure inside the coupling cone. Immediately after exposures, the liver was excised, and boiling histotripsy lesions were produced ex vivo in a separate lobe by using the same exposure parameters. In several cases, the lesions (both in vivo and ex vivo) were bisected and photographed to observe the gross damage to tissue. Otherwise, the liver tissue cuboids of approximately 2 cm^3 containing the lesions were collected, snap frozen, and sectioned longitudinally to the lesion for histological examination.

B-Mode Ultrasound Allows for Treatment Planning, Targeting, and Monitoring in Real Time. The ultrasound imaging system was operated in B mode throughout the HIFU exposure. Because a millimeter-sized boiling bubble is highly reflective for acoustic waves, it is displayed as an echogenic region on grayscale B-mode ultrasound (Fig. 2). First, one probe HIFU pulse was radiated and the appearance of this hyperechoic region was used as an indicator of whether the boiling temperature was reached during one pulse exposure. If the hyperechoic region was not observed, the pulse duration was slightly increased, and the probe pulse was delivered again. This procedure measured the time to boil, t_b, which is an essential parameter for pulsing protocol design. According to our previous findings in ex vivo tissue, the ratio between the time to reach boiling, t_b, and the pulse duration, τ, determines the treatment outcome, along with the duty factor (ratio of the pulse duration and the pulse repetition period) (11, 13). In accordance with theoretical estimations, t_b

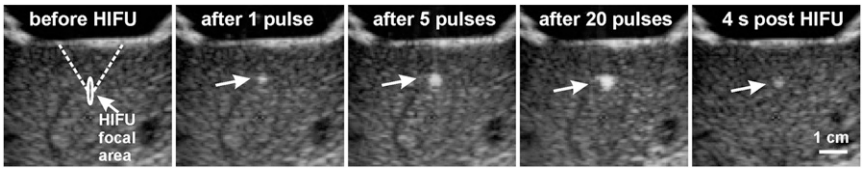

Fig. 2. B-mode ultrasound images taken throughout a boiling-histotripsy exposure. The hypoechoic line at the top of the images corresponds to the interface between the tissue and water-filled coupling cone of the HIFU transducer. The first frame illustrates the position of the HIFU focus inside the liver. The pulsing protocol in this particular case was as follows: HIFU pulse duration 10 ms, pulse repetition frequency 1 s, and treatment duration 50 s. After the first HIFU pulse was delivered, a bright hyperechoic region (indicated by the white arrow) appeared at the HIFU focus. Its brightness was the highest immediately after the pulse was delivered, and decreased slightly before the next pulse arrived. The hyperechoic region continued to grow within the next 20 s of exposure, and then its size saturated. During the subsequent 30 s, the size of the hyperechoic region did not change, which is consistent with our previous observations in ex vivo tissues. After the last HIFU pulse was delivered, the hyperechoic region persisted for several seconds (last frame), but eventually faded completely, and the treated region was indistinguishable from the surrounding tissue. However, the maximum size of the hyperechoic region corresponds well (within the resolution of the ultrasound imaging system) to the size of the resulting lesion (Figs. 3 and 4).

varied within 0.9–1.5 ms, depending on the depth of the focus. Throughout the 50-s exposure, the size and location of the hyperechoic region on the B-mode image corresponded well to the size and location of the resulting lesion, within the resolution of the ultrasound imaging system. Because of the poorer lateral resolution (2.5 mm) compared with the axial resolution (1.5 mm) of the ultrasound image, the hyperechoic region was somewhat distorted (broadened) compared with the resulting lesion (21). The average lesion dimensions, estimated from the histological images, were 6.1 ± 0.5 mm axially and 3.8 ± 0.5 mm laterally, whereas the average hyperechoic region on the ultrasound images, estimated at the mean background brightness level, was 6.5 ± 1.3 mm axially and 6.9 ± 1 mm laterally.

Liquefied Lesion Size, Shape, and Contents Are the Same in Vivo and ex Vivo. The pulsing protocols for ex vivo tissue liquefaction (no thermal damage) developed in our previous work were applied to in vivo and ex vivo porcine liver: The duty factor was kept constant (0.01), while the pulse duration in this set of exposures was varied from 1 ms to 20 ms (t_b -16 t_b) for different treatment locations. All of the exposures resulted in an elongated void of approximately 2 × 4 mm in size, filled with what appeared as liquefied tissue debris and no gross signs of thermal damage, i.e., whitening and thickening of the lesion content (Fig. 3 *A–D*). When the liquefied debris was removed, the lesion wall, both ex vivo and in vivo, displayed the typical structure of individual liver lobules (Fig. 3 *B* and *D*). In our previous work, the effect of structured lesion wall was not observed in ex vivo bovine liver or bovine cardiac muscle (11). This difference is most probably due to the fact that the lobules in porcine liver are separated by thicker connective tissue than those in bovine or human liver, and although the boiling histotripsy exposures destroyed the hepatocyte structure within the lobules, the mechanical disruption of connective tissue was less pronounced. Low magnification histological evaluation of the NADH-stained sections of the liquefied lesions, both in vivo and ex vivo (Fig. 4*A*), confirmed the gross findings. No evidence of thermal damage was observed, i.e., the lesion contents and the tissue at the lesion boundary were stained as intensely as the surrounding tissue. Frozen tissue artifact—large elongated ice crystals aligned in groups—is very pronounced within the lesions, indicating that the contents were indeed liquefied. Connective tissue was not stained by nicotinamide adenine dinucleotide-diaphorase (NADH-d), which enabled observation of the outlines of the lobules in the histological image. As seen in gross observations, the lesion was "contained" by the lobule compartments, and much of the connective tissue immediately adjacent to or within the lesion was not destroyed or damaged. Surprisingly, the magnified view of the NADH-d-stained section of a liquid lesion (Fig. 5*A*) showed a small area of thermal damage confined to the connective tissue within the lesion and to the immediately adjacent hepatocytes. Although this was minor damage compared with the overall lesion volume, this observation indicated that connective tissue may be more susceptible to thermal damage than other tissues. The magnified view of the H&E-stained section of a liquid lesion revealed a very sharply demarcated (1–2 cell lengths or 20–40 μm) lesion border both in vivo and ex vivo (Fig. 5*D*). Most of the tissue debris found within the lesion was no larger than the size of a cell nucleus (3–4 μm) (Fig. 6*A*).

Lysed Red Blood Cells Are Found in the Lesions Produced in Vivo, but Not ex Vivo. Visually, the contents of lesions in ex vivo and in vivo tissue were somewhat different in appearance. The lesions

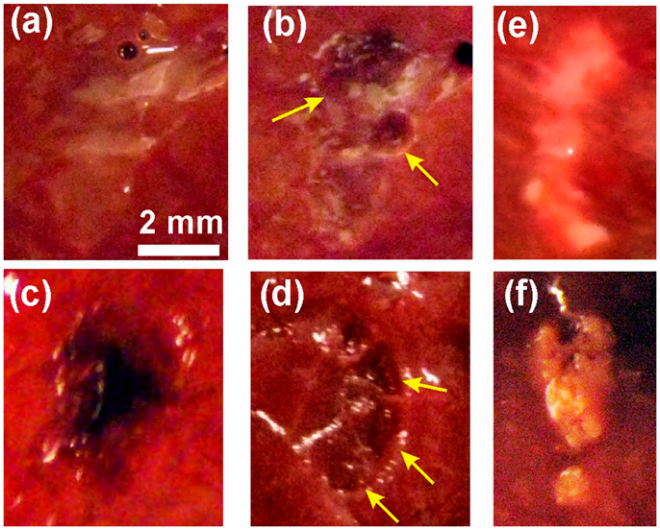

Fig. 3. Representative gross photographs of the boiling-histotripsy lesions induced in ex vivo (*A, B, E,* and *F*) and in vivo (*C* and *D*) porcine liver by using different HIFU pulsing protocols, in which the duty factor was kept constant (0.01) and the HIFU pulse duration varied (1–500 ms). (*A*) When short (less than 20 ms) HIFU pulses were used in the ex vivo setting, the outcome was a void filled with liquid of the same color as surrounding tissue, with no signs of thermal denaturation. The liquid could be easily removed (*B*), and the walls of the remaining cavity repeated the shape of liver lobules (indicated by yellow arrows). The same HIFU treatment delivered in vivo (*C*) created a void of about the same size as ex vivo, but the liquefied contents were much darker and redder than the surrounding tissue. With the contents removed, the lesion structure also repeated the structure of the liver lobules (yellow arrows). (*D*) As the HIFU pulse length increased (20–100 ms) in the ex vivo setting, the lesion contents turned into a thick white paste and the lesion edges were blanched (*E*). In vivo, the thermal damage was not as obvious; the lesion looked essentially the same as the one shown in *C*. With a further increase in pulse duration (100–500 ms), both in vivo and ex vivo, the lesion turned into a well-defined area of coagulative necrosis containing large vacuoles (*F*).

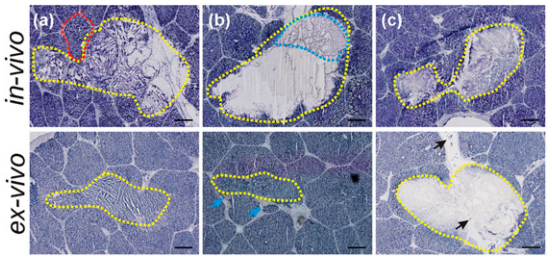

Fig. 4. Representative histological sections of the frozen samples of boiling-histotripsy lesions, produced in in vivo (*Upper*) or ex vivo (*Lower*) porcine liver, stained for NADH-d. The NADH-d stain shows the presence (stained purple) or absence (unstained) of enzymatic activity in tissue, which is used as an indication of thermal damage. Stromal tissue also remains unstained, which allows for visualization of the lobular structure of liver tissue. One of the lobules in *A* is outlined by a red dotted line, and all of the lesions are outlined by dotted yellow lines. (*A*) Liquid lesions produced by using 10-ms-long HIFU pulses. Ice crystal formation in the lesions, both in vivo and ex vivo, indicates that the lesion contents are liquefied. There is no indication of thermal damage, neither to the lesion contents, nor to the surrounding tissue. The higher magnification images stained with H&E (Fig. S6*A*) indicate that the tissue debris within the lesions are no larger than the cell nucleus. The sizes of the in vivo and ex vivo lesions are similar, and the shapes depend on the lobular structure of tissue: The lesions are "contained" by connective tissue, in accord with gross observations. (*B*) "Paste" lesions produced by using longer (100 ms) HIFU pulses. The contents of both lesions are liquefied, but thermal denaturation of the lesion contents occurs to a greater extent in vivo than ex vivo. In vivo, the lesion contents are completely thermally denatured, as are the lesion boundaries within a 100-μm margin. Ex vivo, the thermal effects are confined to the small areas adjacent to the connective tissue (blue arrows). The in vivo lesion also contains a continuous area of thermal necrosis with large vacuoles, outlined with blue dotted line. The size of the intact tissue fragments, contained in both lesions, is larger (up to 50 μm) than in the liquid lesion (Fig. 6*B*). (*C*) Vacuolated thermal lesions produced by using a single 500-ms-long HIFU pulse. The size, structure, and degree of thermal damage are very similar in the in vivo and ex vivo lesions. Both lesions contain thermally necrosed tissue with large vacuoles left by the boiling bubbles. The tissue next to the vacuoles is squeezed and disrupted, whereas closer to the lesion border, it appears thermally fixed. Surprisingly, some of the lesions contain viable cells within the blood vessels, as indicated by the black arrows. (Scale bars: 500 μm.)

produced ex vivo contained liquid that was the same color as surrounding tissue (Fig. 3*A*), whereas the lesions produced in vivo were much darker than surrounding tissue and contained what appeared to be blood (Fig. 3*C*). Upon histological examination, lysed red blood cells (RBCs) were found in abundance in the liquefied lesions produced in vivo (Fig. 5*C*), but were mostly absent in ex vivo samples. It is likely that in vivo, when a small void is formed by the first few HIFU pulses, the leaking of the blood into the void is more intense, compared with the ex vivo case. During the HIFU exposure, most of the red blood cells get lysed, and when the exposure ends, the blood inflow quickly stops, which would explain the absence of intact RBCs.

Large Vessels and Biliary Structures Adjacent to the Lesion Are Resistant to Boiling Histotripsy Damage. If a structure, consisting of mostly connective tissue, e.g., a blood vessel, was located immediately adjacent to the boiling histotripsy-induced liquefied lesion, it was not damaged by the treatment, as illustrated in Fig. 5*A*. This image is also representative of another important observation: Large blood vessels, bile ducts, or other soft tissue inhomogeneities located prefocally in the acoustic path did not interfere with the lesion formation. Similar effects of selective tissue damage caused by ultrasound-mediated therapies have been observed in extracorporeal shock wave lithotripsy (22) and, recently, in cavitation cloud histotripsy as well (23).

Respiratory Tissue Motion Results in Larger Volume of Mechanically Disrupted Tissue. Tissue motion is a challenge in any ablation technique, including boiling histotripsy. If the focal position changes between the sequential HIFU pulses by more than the size of the focal region, several small liquefied voids appear within the focusing range, instead of one large lesion (Fig. 5*B*). However, unlike most thermal ablation methods, boiling histotripsy uses pulses that are short enough to neglect tissue motion within the pulse duration. Therefore, gating the pulses by breathing or cardiac motion will likely solve this problem (3).

Altering HIFU Protocol Causes Similar Degree of Thermal Damage to ex Vivo and in Vivo Tissue. According to our previous experience with other ex vivo tissues, the increase in either HIFU pulse duration or duty factor leads to varying degrees of thermal

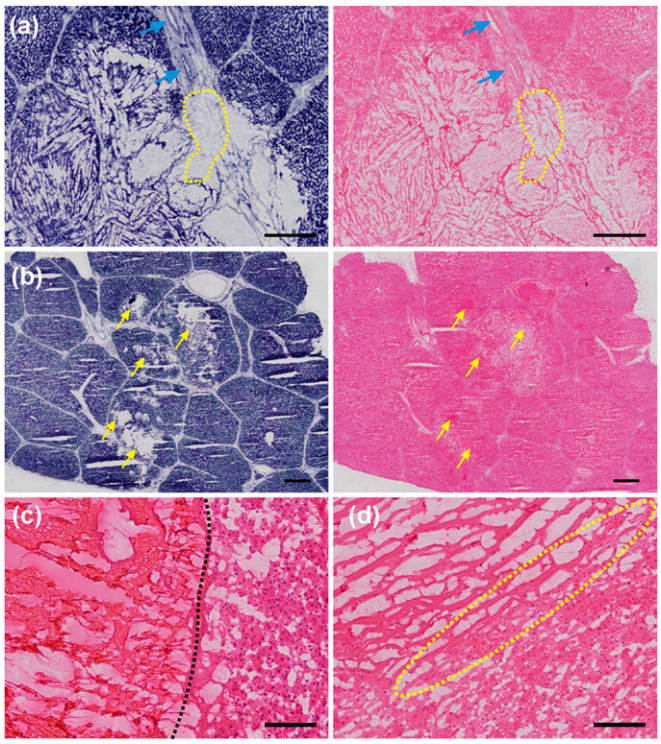

Fig. 5. Higher magnification histological images stained with NADH-d and H&E demonstrating the important details of the liquid lesions produced in vivo by boiling histotripsy. (*A*) H&E (*Left*) and NADH-d (*Right*) stained histological images of a liquid boiling histotripsy lesion. Connective tissue, located within the liquid boiling histotripsy lesions, frequently gets thermally damaged (dotted yellow line), whereas the hepatocytes and the debris thereof are not thermally denatured. If, however, a connective tissue structure (e.g., a blood vessel or a biliary system element) is located immediately adjacent to the lesion, it is not affected (blue arrows) either mechanically or thermally. (*B*) Multifocal boiling-histotripsy lesion produced under the conditions of significant tissue movement due to breathing and heartbeat. The HIFU pulsing protocol used was designed to produce a single liquid lesion (pulse duration 10 ms, pulse repetition frequency 1 Hz, 50-s duration), but because of tissue motion, the HIFU focus location changed from pulse to pulse, and small liquefied areas formed at several places, but did not merge. Tissue motion is a challenge in boiling histotripsy, which can be addressed by gating the HIFU pulses by breathing or cardiac motion. (*C*) Lysed RBCs are abundant in the liquid boiling-histotripsy lesions and are seen in the H&E-stained sections of the lesions as a red tint (left side of the image). Intact RBCs were not observed within the lesions, indicating that the blood inflow to the emulsified void continued only through the HIFU exposure and stopped shortly afterward. (*D*) High magnification H&E stained image of the liquid lesion border, which is very sharp and only one to two cells (10–20 μm) in width. (Scale bars: *A* and *B*, 500 μm; *C*, 100 μm.)

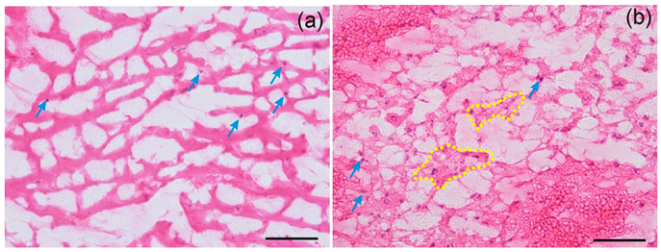

Fig. 6. Magnified view of the H&E-stained histological sections of the debris contained in liquid (*A*) and paste (*B*) lesions produced in vivo. Ice crystal formation is pronounced in both images, indicating that the lesion contents is mostly liquefied. Both lesions contain a few intact cell nuclei (blue arrows), that are much more abundant in the paste lesion. The latter also contains larger tissue fragments, up to 100 μm in size, outlined by yellow dotted lines. (Scale bars: 50 μm.)

damage to tissue due to heat accumulation (11, 13). In the present study, thermal denaturation of both ex vivo and in vivo porcine liver was observed with an increase in HIFU pulse duration up to 100 ms or ~80 t_b. Fig. 3*E* shows a gross view of a lesion produced by 100-ms HIFU pulses. The lesion shape and size did not change noticeably compared with the tissue liquefaction regime, but the contents turned into white, thermally denatured paste in the ex vivo setting, and the edges of the lesion became blanched. In the in vivo case, the thermal damage was not obvious by gross observation because of the presence of circulation and the dark background of coagulated blood in the lesion. The general appearance of the lesion was similar to the liquid lesion shown in Fig. 3*C*. NADH-d stained histological sections (Fig. 4*B*) of such "paste" lesions in vivo indicated that both the cellular structure of the hepatocytes and the connective tissue were completely destroyed, and the resulting debris were thermally denatured, yet retained a liquid consistency. In the ex vivo case, the thermal damage was confined to regions close to the connective tissue separating the lobules, and did not involve the cellular debris of the hepatocytes themselves, which was consistent with the observations in liquid lesions. This difference can be explained by the lack of circulation and, consequently, a greater heat deposition in the septal regions. In both cases, the paste lesions were not as confined by connective tissue as the liquid lesions, possibly due to heat-induced denaturation of the connective tissue. The size of the tissue debris in the paste lesion both in vivo and ex vivo was larger (up to 100 μm) than the size of the debris in the liquid lesion (Fig. 6*B*).

Further increase of the HIFU pulse length led to the formation of a solid thermal lesion with large vacuoles left from the boiling bubbles, both in vivo and ex vivo (Fig. 3*F*). This type of lesion will be referred to as "vacuolated thermal." According to the histological images stained with NADH-d (Fig. 4*C*), thermal denaturation of the tissue within the lesion was complete, in both in vivo and ex vivo cases.

Discussion

The boiling histotripsy method offers a unique capability to locally fractionate (liquefy) bulk tissue into fragments smaller than the cell nucleus. We have demonstrated here, to our knowledge for the first time, that this method is successful in producing liquefied lesions in vivo. We have performed these experiments in bulk porcine liver tissue under diagnostic ultrasound guidance and monitoring and found that the treatment outcome, e.g., the degree of tissue fractionation and thermal damage in the lesion, and the lesion size and shape thereof, was generally very similar in in vivo and ex vivo tissue. Certain differences, such as the presence of lysed RBCs in the lesion in vivo, were identified and related to the presence of circulation in the in vivo case.

The single lesions that were produced here were roughly 2 mm × 3 mm in size, whereas in the clinically relevant ablation applications, the volume of tissue to be removed is much larger. The larger ablation volume can be achieved by steering the HIFU focus, either mechanically or electronically, over the desired area, and all of the commercially available HIFU arrays offer that option (19). Moreover, as shown in our previous ex vivo experiments, the size of a single liquefied lesion is inversely proportional to the HIFU frequency and can, therefore, be controlled by the choice of this parameter (8).

As seen from the results of both ex vivo and in vivo experiments, connective tissue is much more resistant to the mechanical damage produced by boiling histotripsy than other tissue types, most probably due to the high tensile strength of the collagen present in the septum, which makes it difficult to mechanically damage this region. This effect is certainly a drawback if cutting through connective tissue is the desired outcome, but in the situation for which the structures next to the target (such as a blood vessel, tumor capsule, or organ lining) are to be spared, it can be a distinct advantage.

The extent of thermal effects induced by different boiling histotripsy pulsing protocols was shown to be consistent between ex vivo and in vivo tissue of the same type. This observation provides a great opportunity to use exposures in the ex vivo tissue as a validated substitute for some of the preliminary in vivo experiments. Interestingly, the thermal damage to porcine kidney in this study was observed at much longer HIFU pulse durations (40 t_b) compared with the pulse durations that were sufficient to induce thermal denaturation in ex vivo bovine heart or liver tissue considered in our previous studies (5 t_b) (13), which demonstrates that vivo histotripsy protocol design is tissue specific.

We have successfully used conventional B-mode ultrasound imaging for targeting and monitoring the boiling histotripsy treatment. The maximum size of the hyperechoic region seen at the focus during the exposure corresponded well (within the resolution limit of the imaging system) to the size of the resulting lesion. The lesion itself could not be visualized by the imaging system, but this may be due to insufficient spatial resolution provided by the probe that was used in the study. The use of higher frequency, linear array probes would likely solve that problem.

Overall, with the use of multielement HIFU arrays for rapid beam steering, and higher frequency ultrasound probes for treatment guidance and monitoring, boiling histotripsy can become a powerful ablation technique. As the use of HIFU becomes more and more accepted as an important clinical treatment for a number of pathologies and medical conditions, boiling histotripsy is an approach that can utilize existing commercial clinical systems while addressing the important limitations facing the increased use of focused ultrasound for therapy. In particular, the use of diagnostic ultrasound instead of MR thermometry will dramatically decrease the cost of the procedure. Unlike thermal ablation techniques, boiling histotripsy is not affected by the heat-sink effect of the large blood vessels and, due to tissue selectivity, is capable of treating the immediately adjacent tissue. Thermal effects on the intervening tissues—heating of the ribs and skin burns, which are important problems in conventional HIFU treatments—are also avoided in boiling histotripsy.

Methods

HIFU Pulsing Protocol Design. In this study, the HIFU transducer was operated at the peak acoustic output power of 240 W, in a pulsed regime (Fig. S1). At this output power, the amplitude of the shock front that forms at the focus in tissue is 87–102 MPa, depending on the depth of focus location. The corresponding time to reach boiling temperature, according to weak shock theory, is then 0.9–1.2 ms (12). According to our previous findings in ex vivo tissue, the duty factor (ratio of the pulse duration and the pulse repetition period) and the ratio between the time to reach boiling, t_b, and the pulse

duration determine the treatment outcome (11, 13). To find the correlation between HIFU parameter space and treatment outcome in vivo (in terms of the degree of thermal damage to tissue and tissue fractionation), different pulsing schemes were used. Total exposure time (50 s) and duty factor (0.01) were kept constant while changing the HIFU pulse duration within a 1-ms to 500-ms range (1–500 t_b), more specifically: 1, 2, 5, 10, 20, 50, 100, and 500 ms (seven different exposure protocols total).

Animal Experiments. All procedures in the animal experiments followed the protocols approved by the Institutional Animal Care and Use Committee at the University of Washington. The animals were housed in a facility at the University of Washington that is fully accredited by the Association for Assessment and Accreditation of Laboratory Animal Care International. The animals were cared for by a full-time veterinary staff. Before each experiment, the animal was anesthetized with Telazol premedication and then masked with isoflurane. Thereupon the liver was exteriorized and 2–5 HIFU exposures thereof were performed. The animal was euthanized immediately after the HIFU exposures were complete, and the liver was excised.

In vivo HIFU exposures were performed in 12 pigs. In two animals, the resulting lesions were examined grossly (n = 1–2 per each of the seven exposure protocols). In 10 animals, the lesions were collected for histology. At each experiment, several (2–4) different HIFU exposure protocols were randomly chosen, so that overall n = 4 histological samples of each of the seven exposure protocols were collected.

Additional HIFU sonications were induced ex vivo in two freshly excised porcine livers. Per each exposure protocol, n = 3 samples were collected for histology and one sample examined grossly and photographed.

Preparation of the Histological Samples. Sequential 8-μm-thick slices were collected from the middle of each lesion, and one of the sections was stained with hematoxylin and eosin (H&E). Hematoxylin stains the cell nuclei blue/purple, whereas eosin stains the cytoplasm, connective tissue, and other extracellular substances pink or red, thus allowing the visualization of tissue structure and its mechanical disruption. The other section was stained for NADH-d activity to evaluate the extent of thermal damage. In this enzyme histological stain, tissue that contains active NADH-d (an enzyme produced by mitochondria) is stained blue/purple and is considered viable, whereas thermally killed tissue remains unstained. The NADH-d stain is routinely used in evaluation of the results of RF ablation (24).

ACKNOWLEDGMENTS. We thank Dr. Peter Kazckowski for his input in design, fabrication, and characterization of the HIFU transducer array used in this study. This work was sponsored in part by National Institute of Health Grants R01 DK43881, R01 EB0007643, and K01 EB015745 and by the National Space Biomedical Research Institute through NASA NCC 9-58.

1. Dubinsky TJ, Cuevas C, Dighe MK, Kolokythas O, Hwang JH (2008) High-intensity focused ultrasound: Current potential and oncologic applications. *AJR Am J Roentgenol* 190(1):191–199.
2. Bailey MR, Khokhlova VA, Sapozhnikov OA, Kargl SG, Crum LA (2003) Physical mechanisms of the therapeutic effect of ultrasound (a review). *Acoust Phys* 49: 369–388.
3. Leslie T, et al. (2012) High-intensity focused ultrasound treatment of liver tumours: Post-treatment MRI correlates well with intra-operative estimates of treatment volume. *Br J Radiol* 85(1018):1363–1370.
4. Crouzet S, et al. (2014) Whole-gland ablation of localized prostate cancer with high-intensity focused ultrasound: Oncologic outcomes and morbidity in 1002 patients. *Eur Urol* 65(5):907–914.
5. Ren XL, et al. (2007) Extracorporeal ablation of uterine fibroids with high-intensity focused ultrasound: Imaging and histopathologic evaluation. *J Ultrasound Med* 26(2): 201–212.
6. Khokhlova TD, Hwang JH (2011) HIFU for palliative treatment of pancreatic cancer. *J Gastrointest Oncol* 2(3):175–184.
7. Elias WJ, et al. (2013) A pilot study of focused ultrasound thalamotomy for essential tremor. *N Engl J Med* 369(7):640–648.
8. Jolesz FA, Hynynen K, McDannold N, Tempany C (2005) MR imaging-controlled focused ultrasound ablation: A noninvasive image-guided surgery. *Magn Reson Imaging Clin N Am* 13(3):545–560.
9. Etame AB, et al. (2012) Focused ultrasound disruption of the blood-brain barrier: A new frontier for therapeutic delivery in molecular neurooncology. *Neurosurg Focus* 32(1):E3.
10. Mo S, Coussios CC, Seymour L, Carlisle R (2012) Ultrasound-enhanced drug delivery for cancer. *Expert Opin Drug Deliv* 9(12):1525–1538.
11. Khokhlova TD, et al. (2011) Controlled tissue emulsification produced by high intensity focused ultrasound shock waves and millisecond boiling. *J Acoust Soc Am* 130(5):3498–3510.
12. Canney MS, Khokhlova VA, Bessonova OV, Bailey MR, Crum LA (2010) Shock-induced heating and millisecond boiling in gels and tissue due to high intensity focused ultrasound. *Ultrasound Med Biol* 36(2):250–267.
13. Wang YN, Khokhlova T, Bailey M, Hwang JH, Khokhlova V (2013) Histological and biochemical analysis of mechanical and thermal bioeffects in boiling histotripsy lesions induced by high intensity focused ultrasound. *Ultrasound Med Biol* 39(3): 424–438.
14. Simon JC, et al. (2012) Ultrasonic atomization of tissue and its role in tissue fractionation by high intensity focused ultrasound. *Phys Med Biol* 57(23):8061–8078.
15. Parsons JE, Cain CA, Abrams GD, Fowlkes JB (2006) Pulsed cavitational ultrasound therapy for controlled tissue homogenization. *Ultrasound Med Biol* 32(1):115–129.
16. Roberts WW, et al. (2006) Pulsed cavitational ultrasound: A noninvasive technology for controlled tissue ablation (histotripsy) in the rabbit kidney. *J Urol* 175(2):734–738.
17. Hall TL, et al. (2009) Histotripsy of the prostate: Dose effects in a chronic canine model. *Urology* 74(4):932–937.
18. Vlaisavljevich E, et al. (2013) Image-guided non-invasive ultrasound liver ablation using histotripsy: Feasibility study in an in vivo porcine model. *Ultrasound Med Biol* 39(8):1398–1409.
19. Yuldashev PV, et al. (2013) Characterization of a multi-element clinical HIFU system using acoustic holography and nonlinear modeling. *IEEE Trans. Ultrason. Ferr. Freq. Control.* 60:1683–1698.
20. Maxwell A, et al. (2012) Disintegration of tissue using high intensity focused ultrasound: Two approaches that utilize shock waves. *Acoustics Today* 8(12):24–37.
21. Hill CR, Bamber JC, ter Haar G (2004) *Physical Principles of Medical Ultrasonics* (Wiley, West Sussex, UK), Chap 9, 2nd Ed.
22. Evan AP, Willis LR, Lingeman JE, McAteer JA (1998) Renal trauma and the risk of long-term complications in shock wave lithotripsy. *Nephron* 78(1):1–8.
23. Vlaisavljevich E, et al. (2014) Effects of tissue mechanical properties on susceptibility to histotripsy-induced tissue damage. *Phys Med Biol* 59(2):253–270.
24. Date RS, et al. (2005) Development and validation of an experimental model for the assessment of radiofrequency ablation of pancreatic parenchyma. *Pancreas* 30(3): 266–271.

Supporting Information

Khokhlova et al. 10.1073/pnas.1318355111

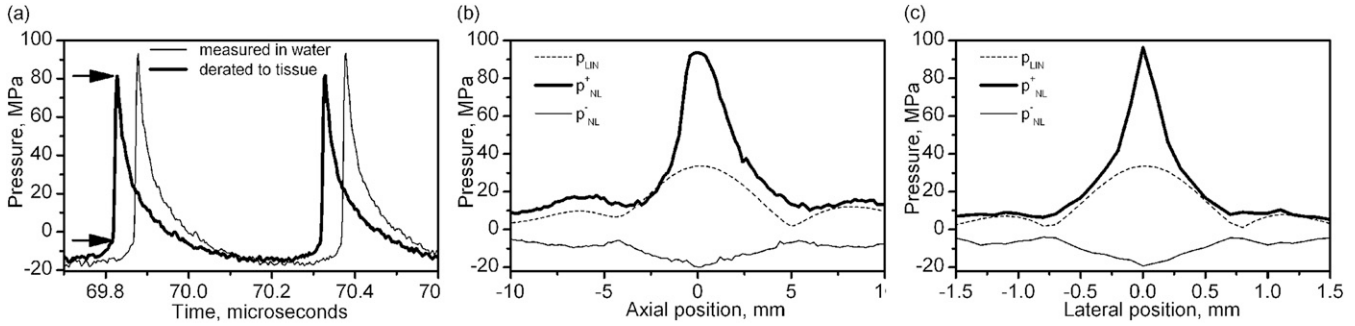

Fig. S1. Characterization of the high intensity focused ultrasound (HIFU) field at 240 W power of the transducer used for boiling histotripsy sonications: (*A*) The focal ultrasound waveform measured in water by the fiber-optic pressure hydrophone (thin line) and derated to tissue (thick line) for 18 mm depth of focus location. The derating procedure accounted for higher ultrasound attenuation (0.08 Np/cm) and higher nonlinearity parameter (equal to 4) in tissue compared with water (1). The shock front of the in situ waveform is marked by the arrows, and its amplitude in this case was 87 MPa. The shock amplitude determines the time to boil in tissue, which was 1.5 ms, as calculated by using weak shock theory. The distribution of peak positive (thick line, p_{NL}^+) and peak negative (thin line, p_{NL}^-) pressures along (*B*) and across (*C*) the focal area of the HIFU transducer were measured in water by scanning the fiber-optic pressure hydrophone. Point "0" corresponds to the focus location. Sharp focusing for the peak positive pressure, which mainly determines the shock amplitude, explains highly localized heating by shocks. The dotted lines show the pressure distribution assuming linear propagation regime, p_{LIN}, given the same ultrasound intensity at the focus, for comparison.

1. Khokhlova TD, et al. (2011) Controlled tissue emulsification produced by high intensity focused ultrasound shock waves and millisecond boiling. *J Acoust Soc Am* 130(5):3498–3510.

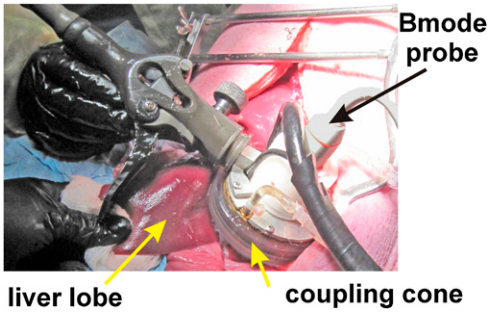

Fig. S2. A photograph of the experimental arrangement.